

## **Supplemental Material to:**

**Mi-Hyang Cho, Kwangmin Cho, Hoe-Jin Kang,  
Eun-Young Jeon, Hun-Sik Kim, Hyung-Joon Kwon,  
Hong-Mi Kim, Dong-Hou Kim, and Seung-Yong Yoon**

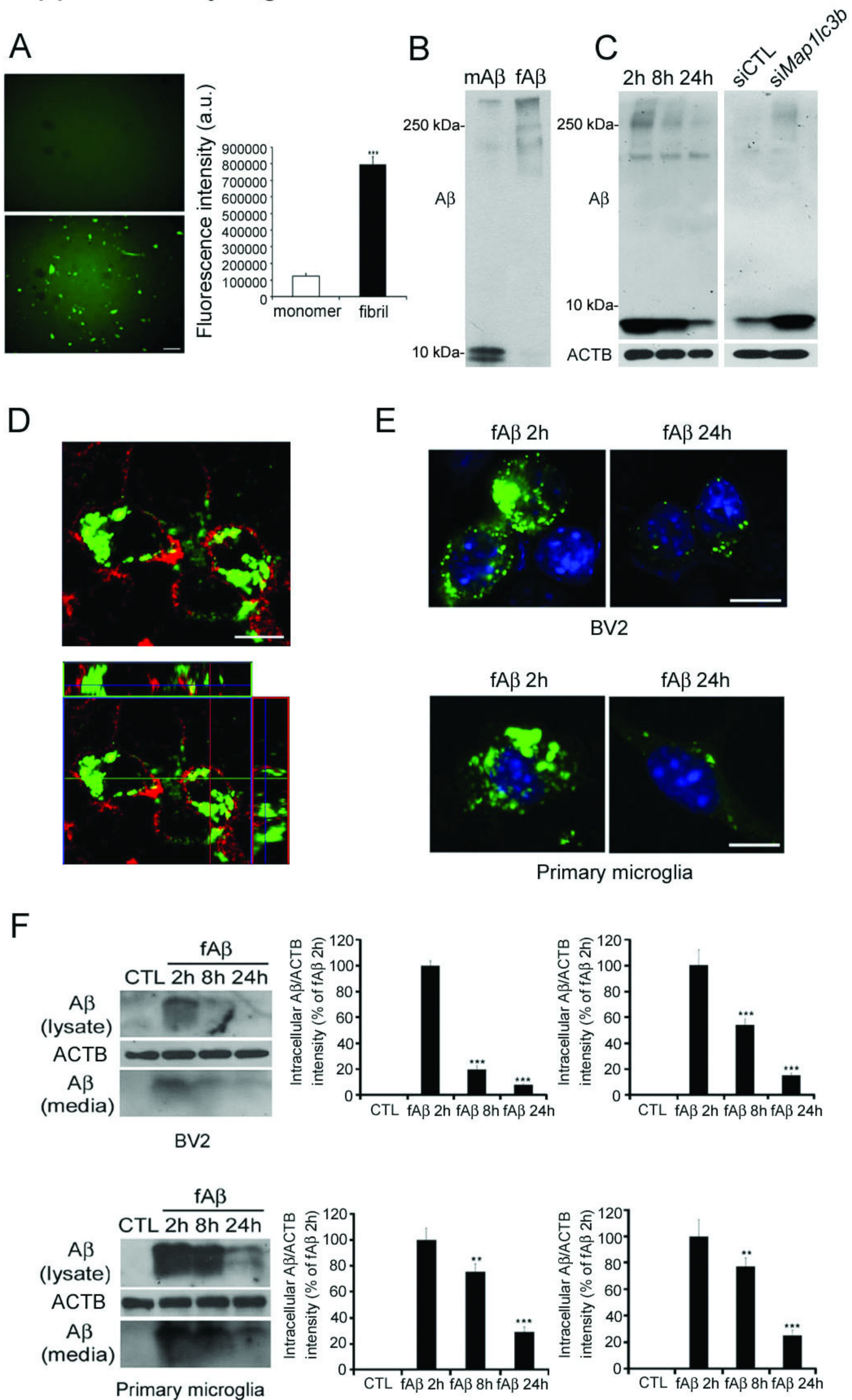
**Autophagy in microglia degrades extracellular  $\beta$ -amyloid  
fibrils and regulates the NLRP3 inflammasome**

**Autophagy 2014; 10(10)**

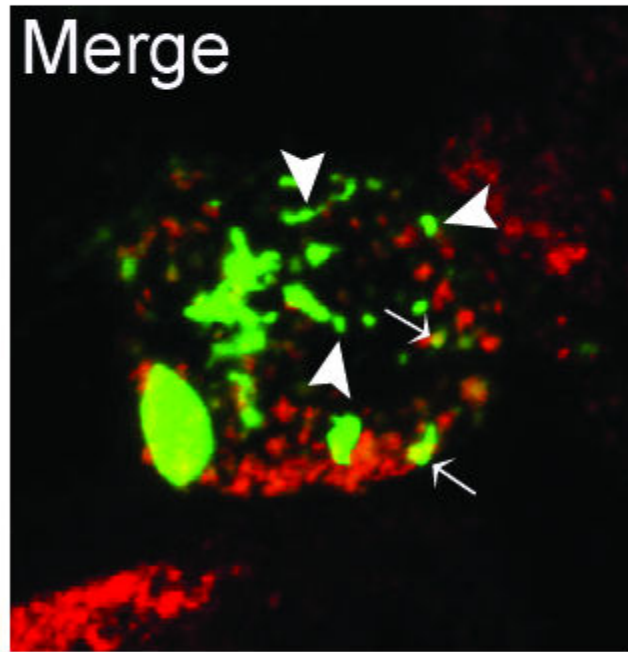
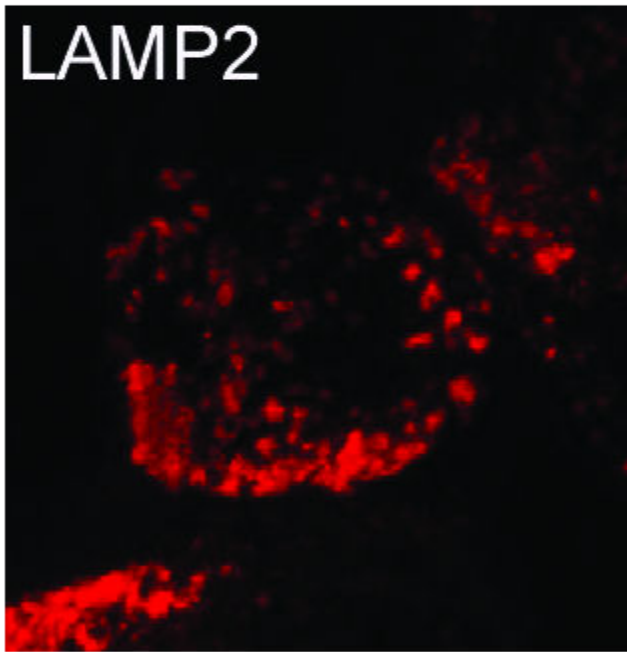
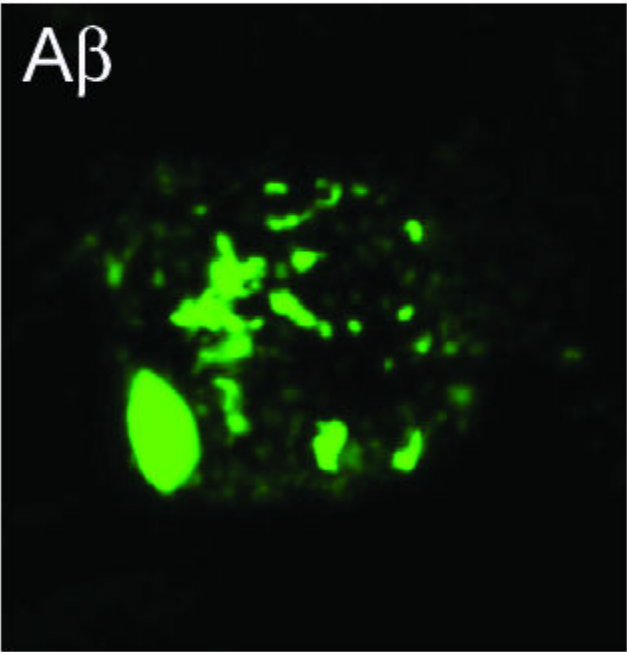
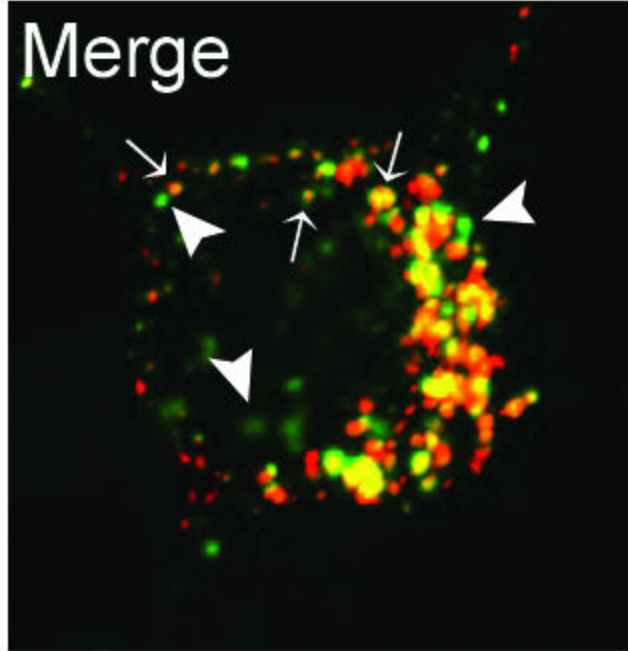
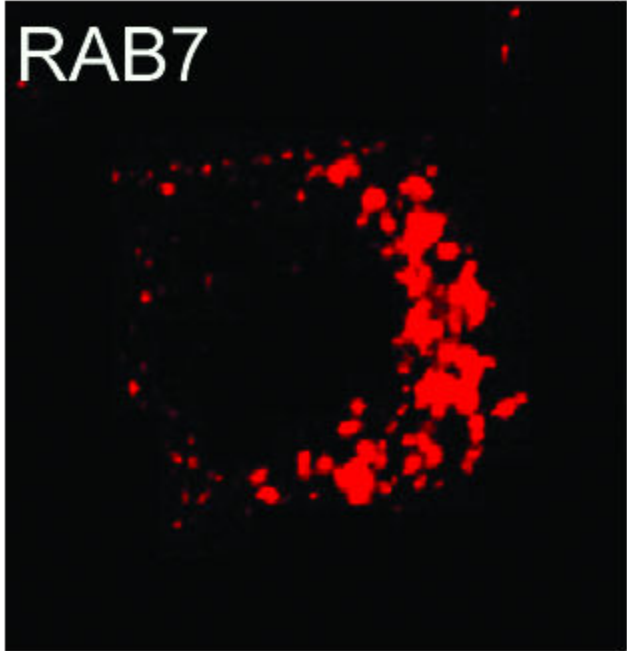
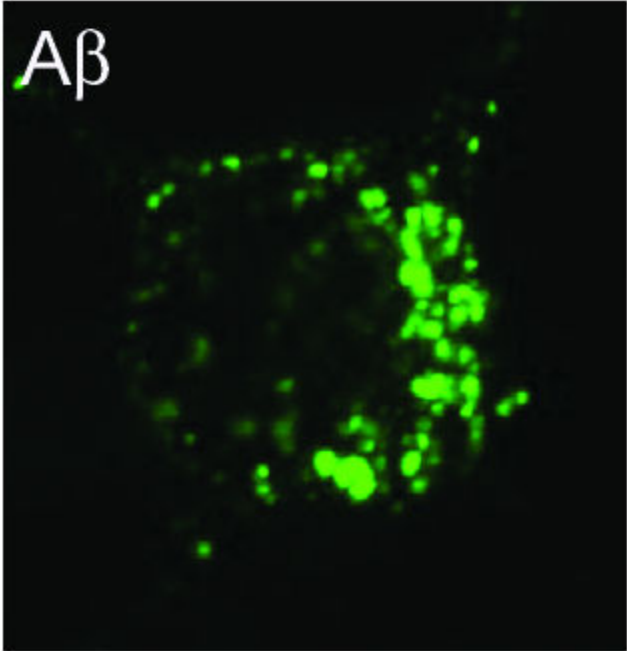
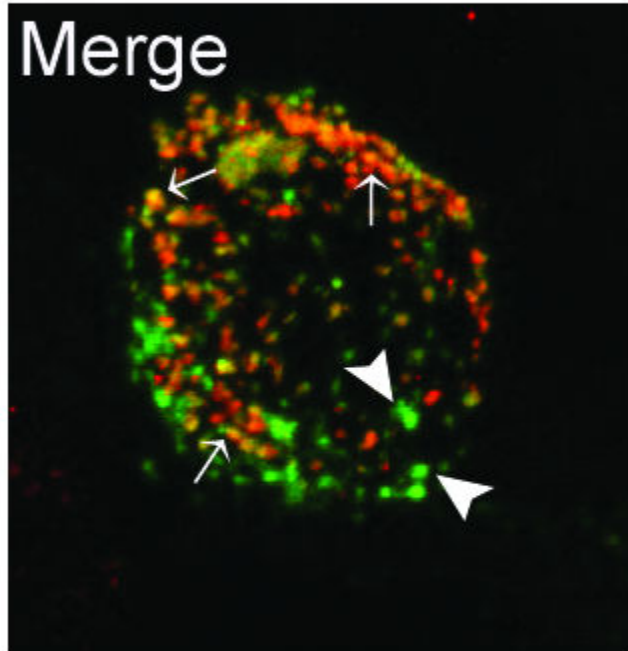
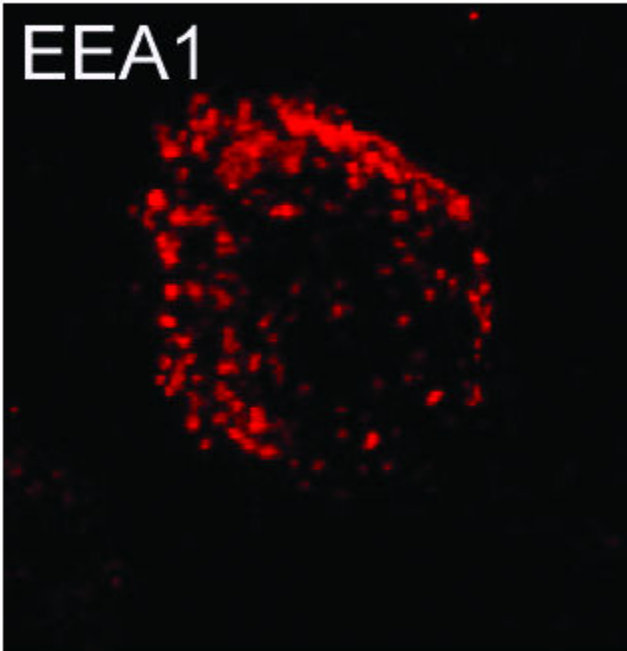
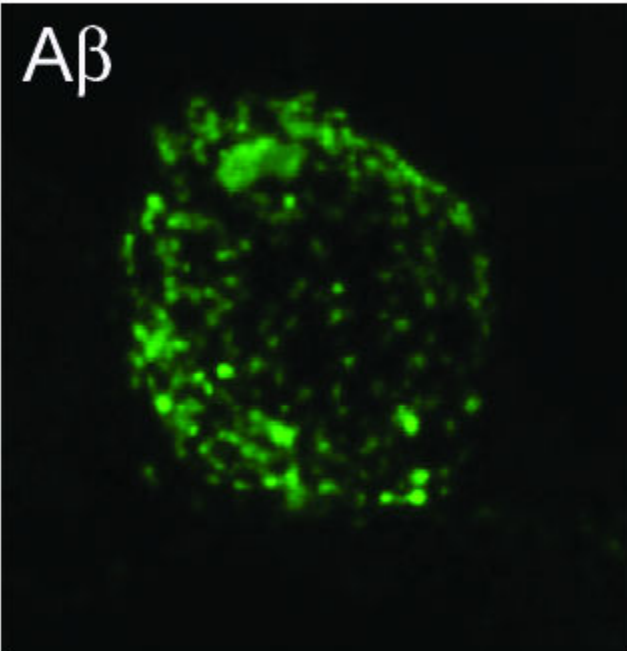
**<http://dx.doi.org/10.4161/auto.29647>**

**[www.landesbioscience.com/journals/autophagy/article/29647](http://www.landesbioscience.com/journals/autophagy/article/29647)**

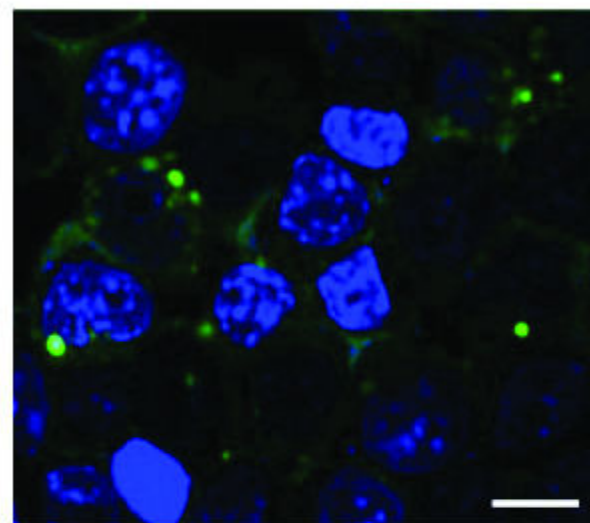
# Supplementary Figure S1.



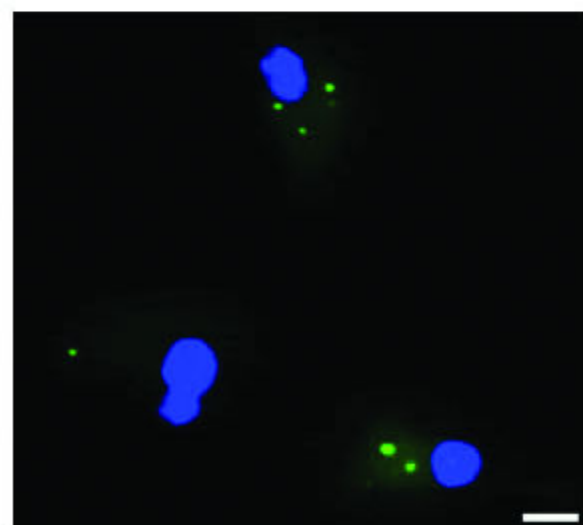
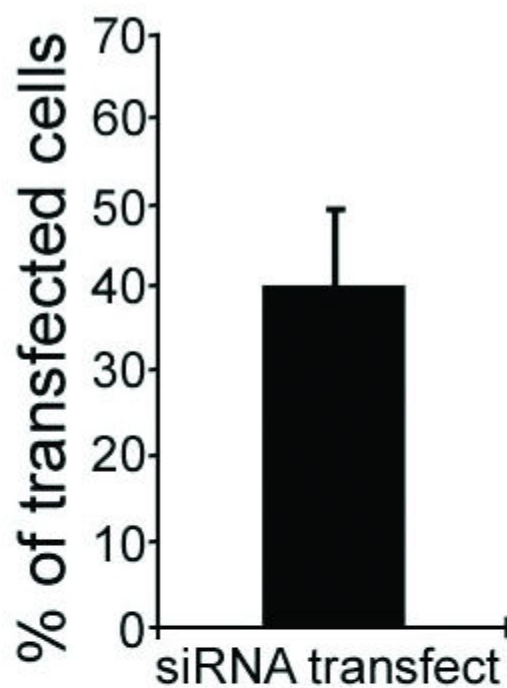
Supplementary Figure S2.



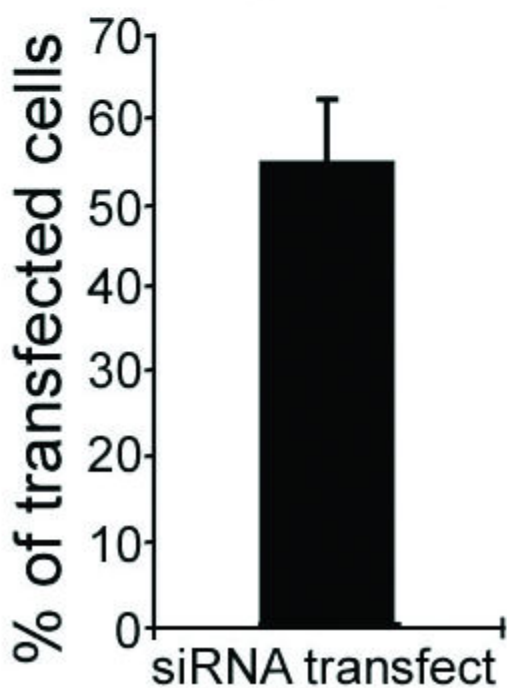
# Supplementary Figure S3.



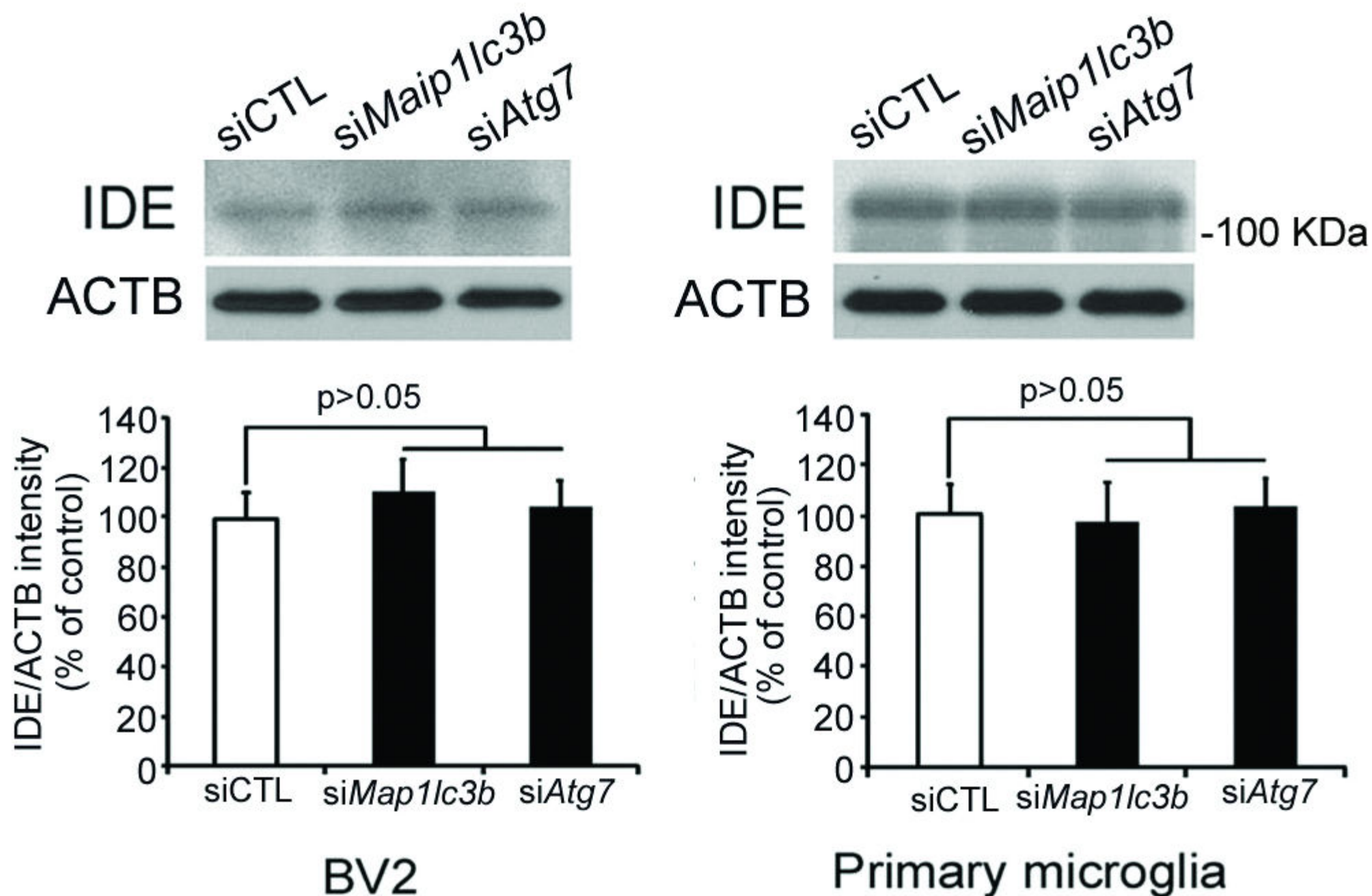
BV2



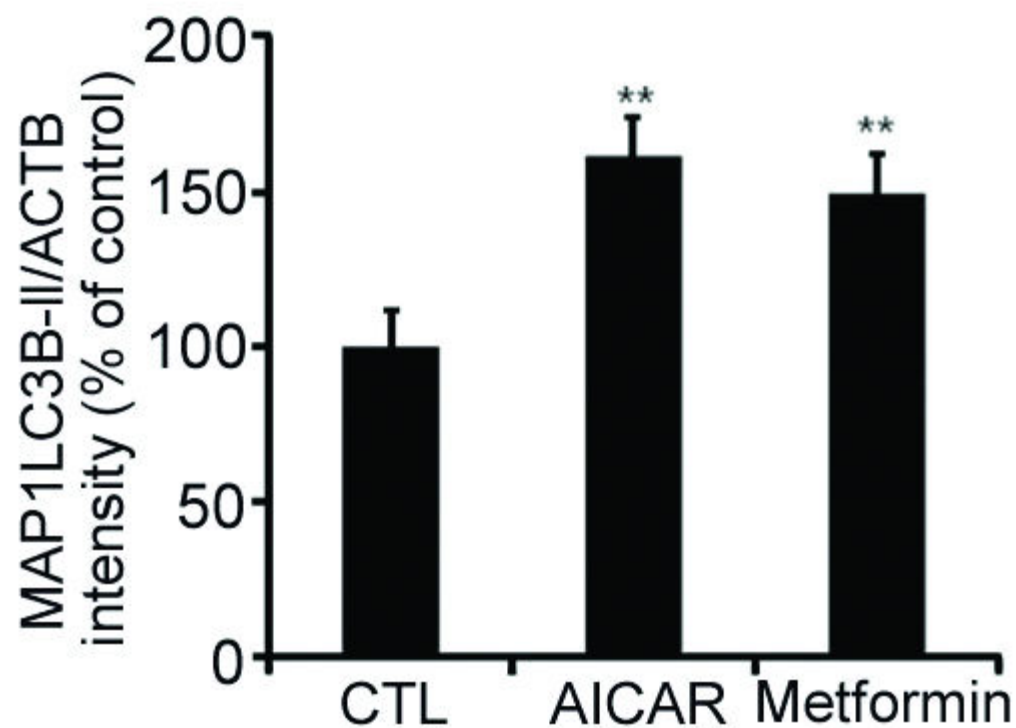
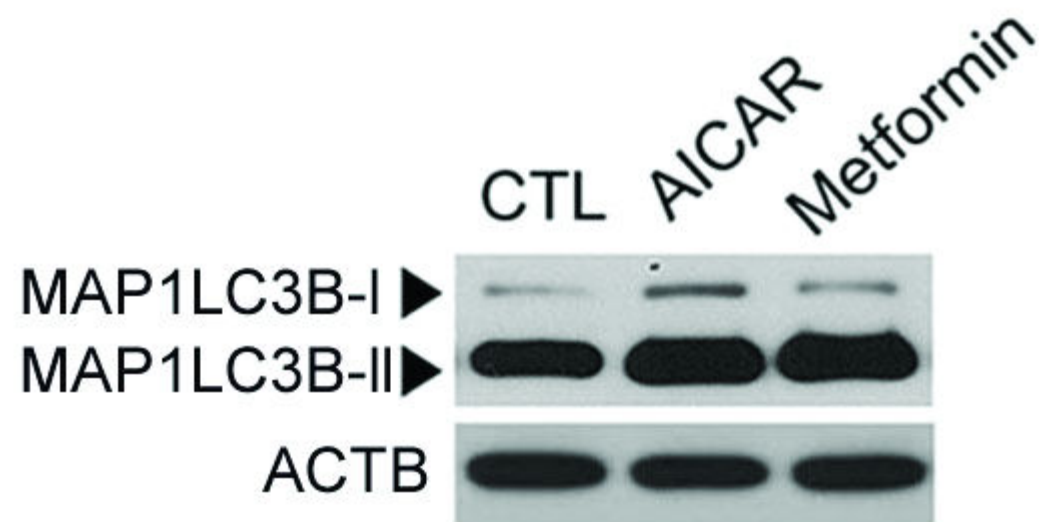
Primary microglia



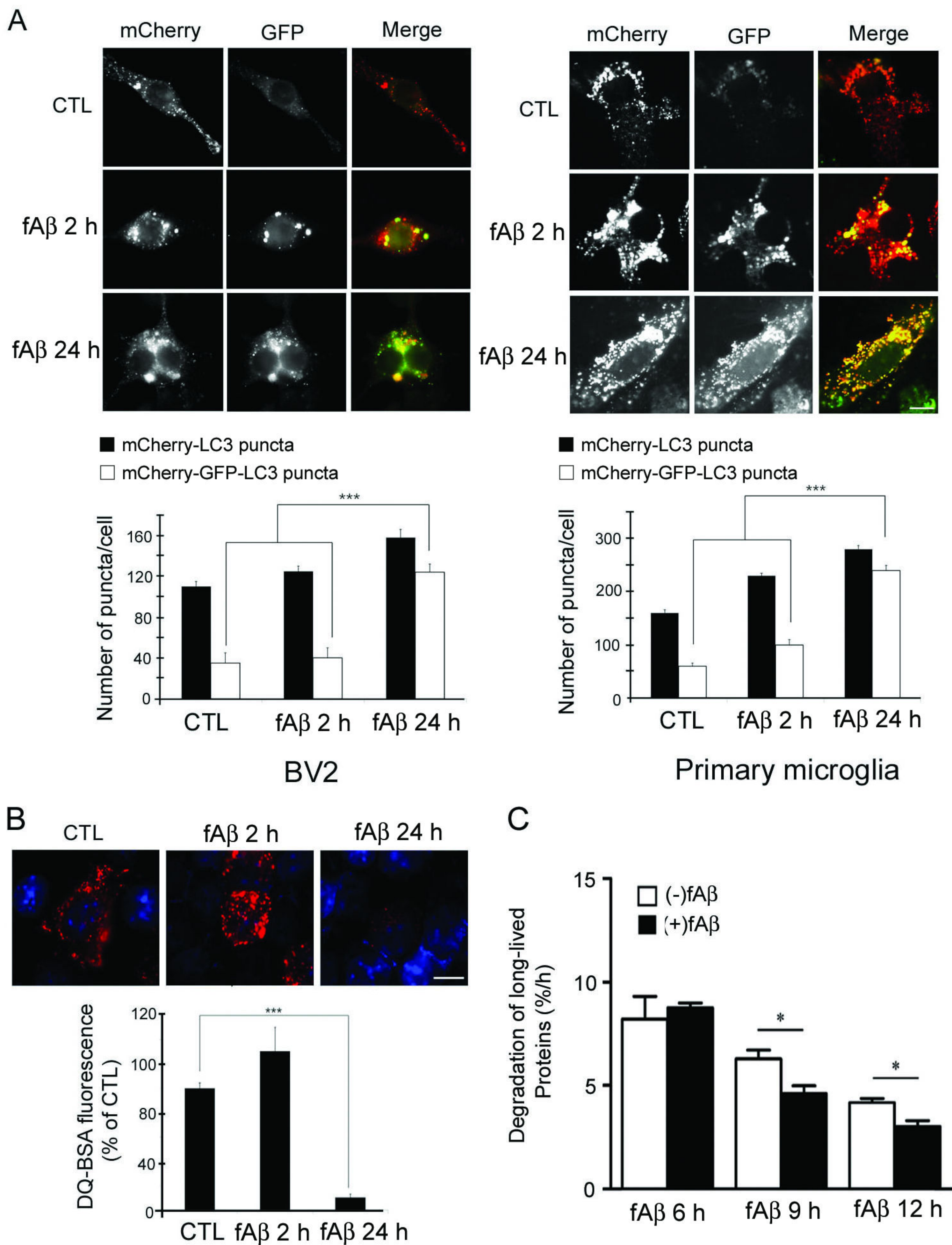
## Supplementary Figure S4.



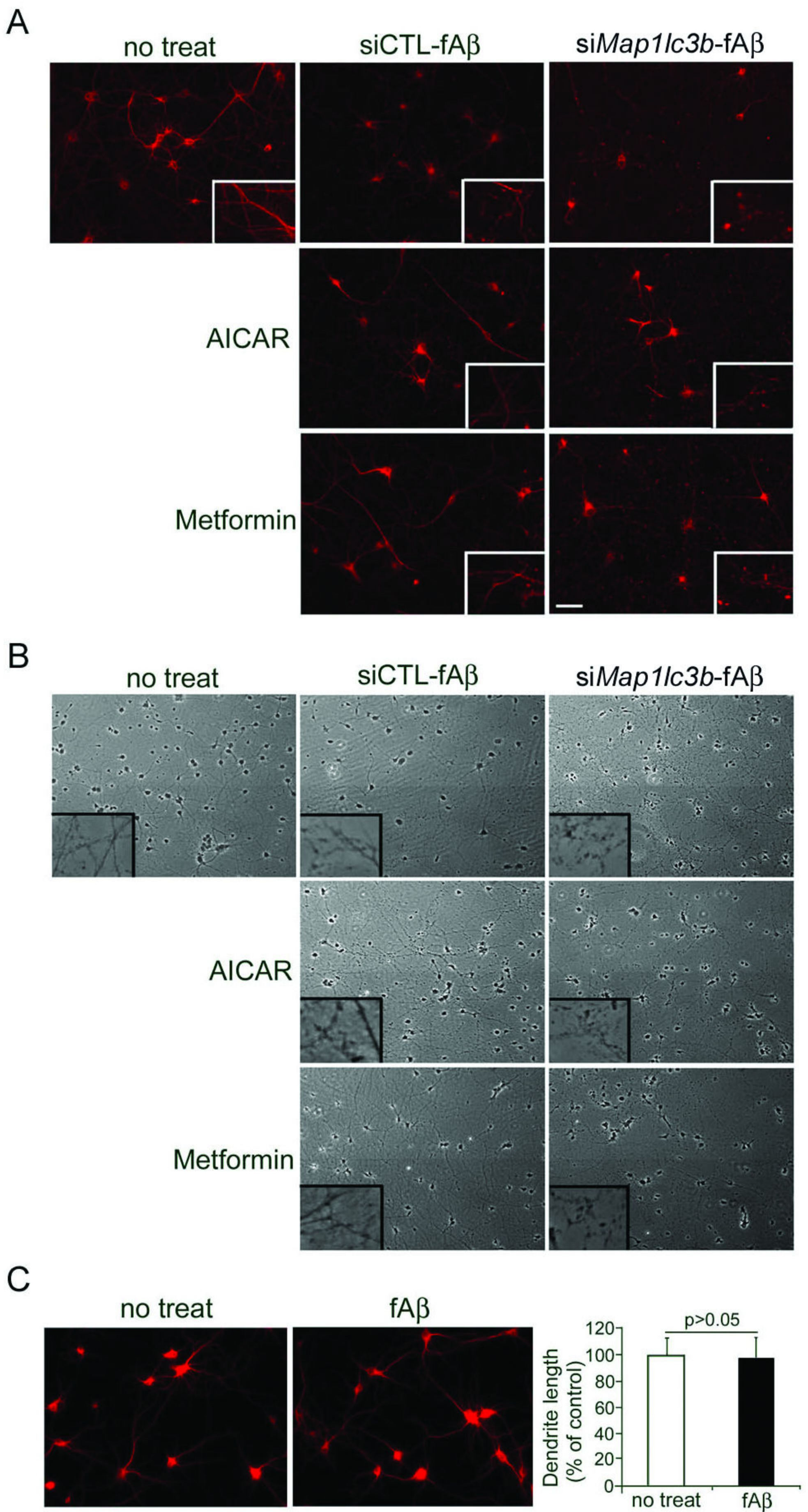
## Supplementary Figure S5.



# Supplementary Figure S6.

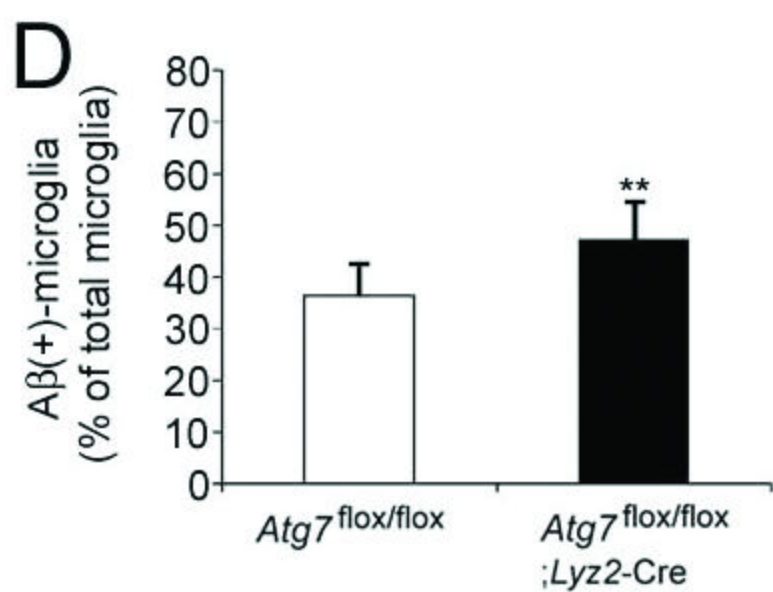
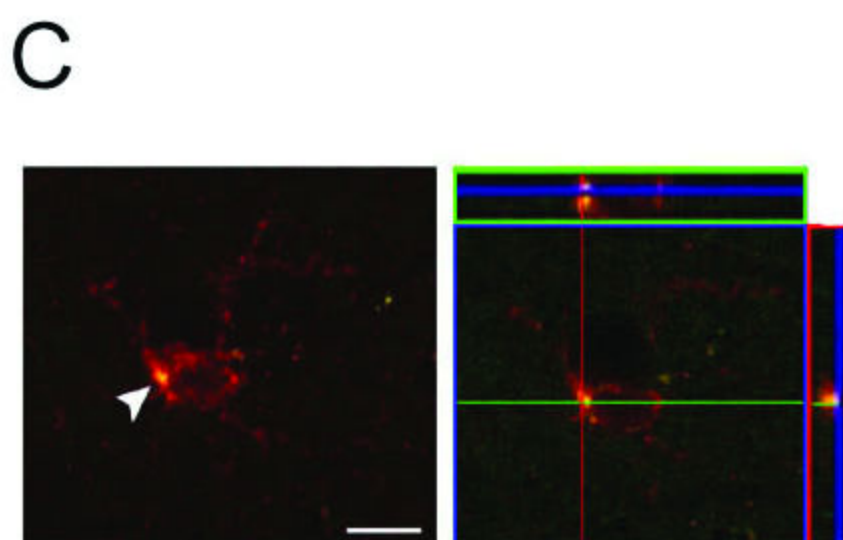
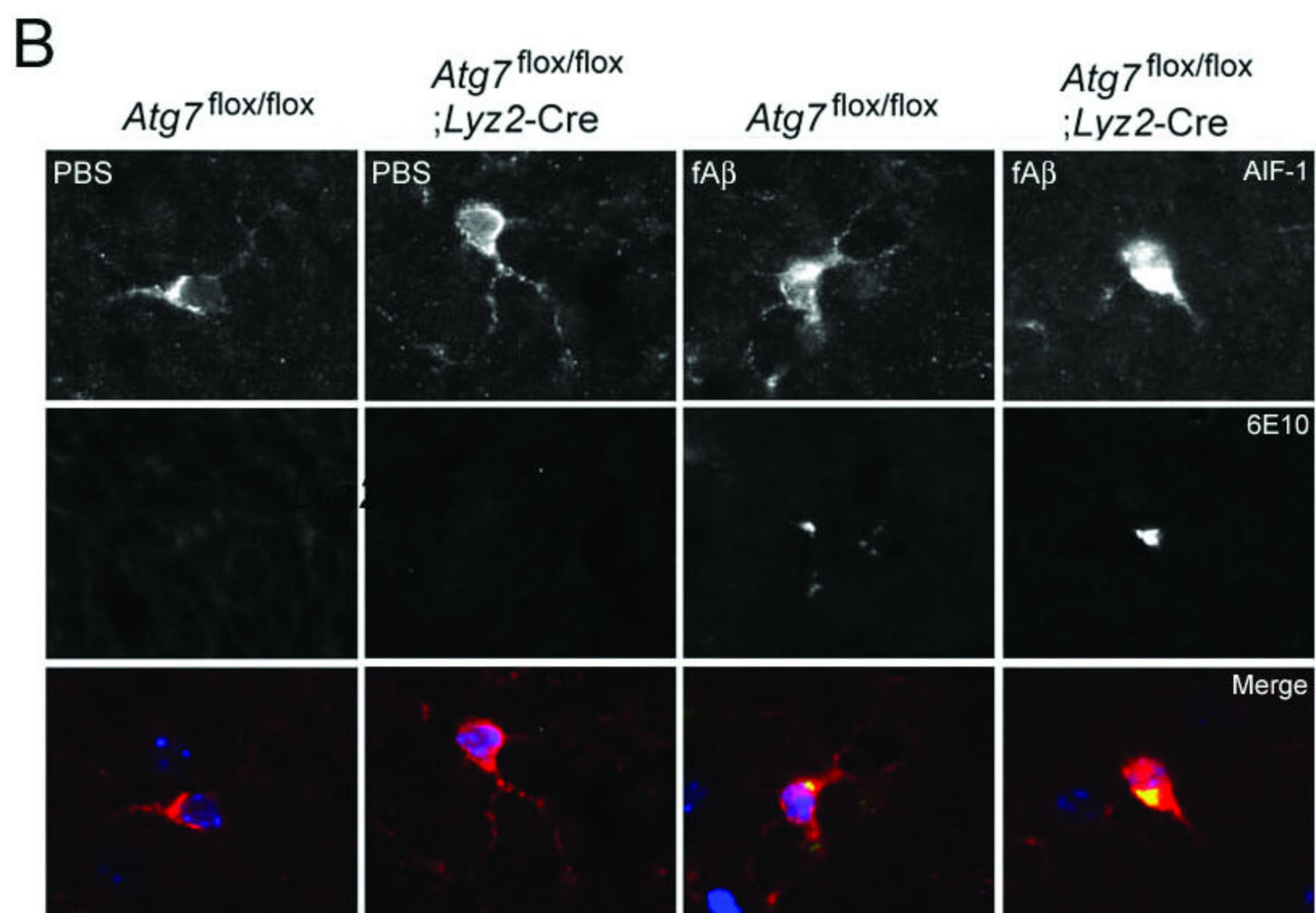
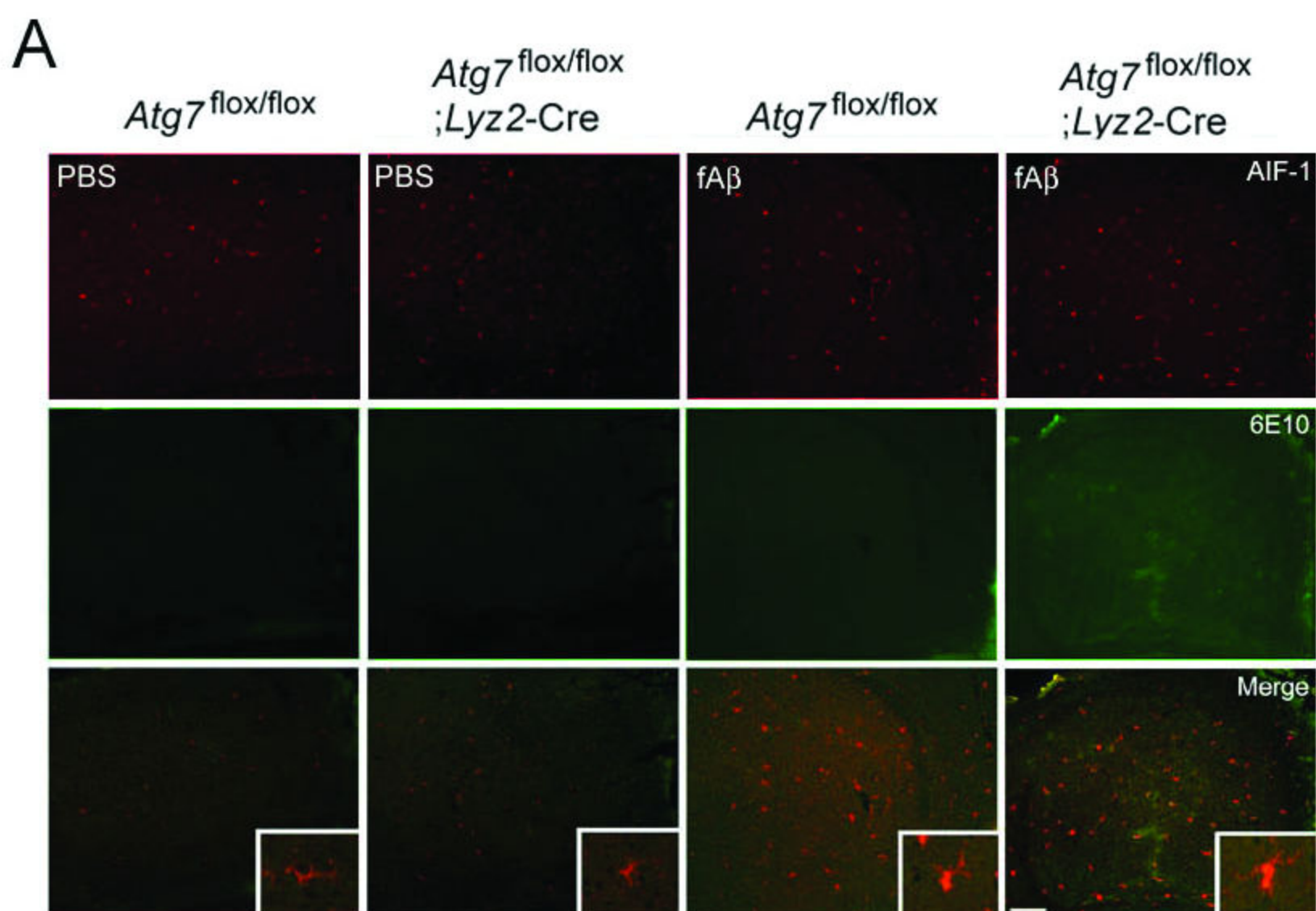


# Supplementary Figure S7.



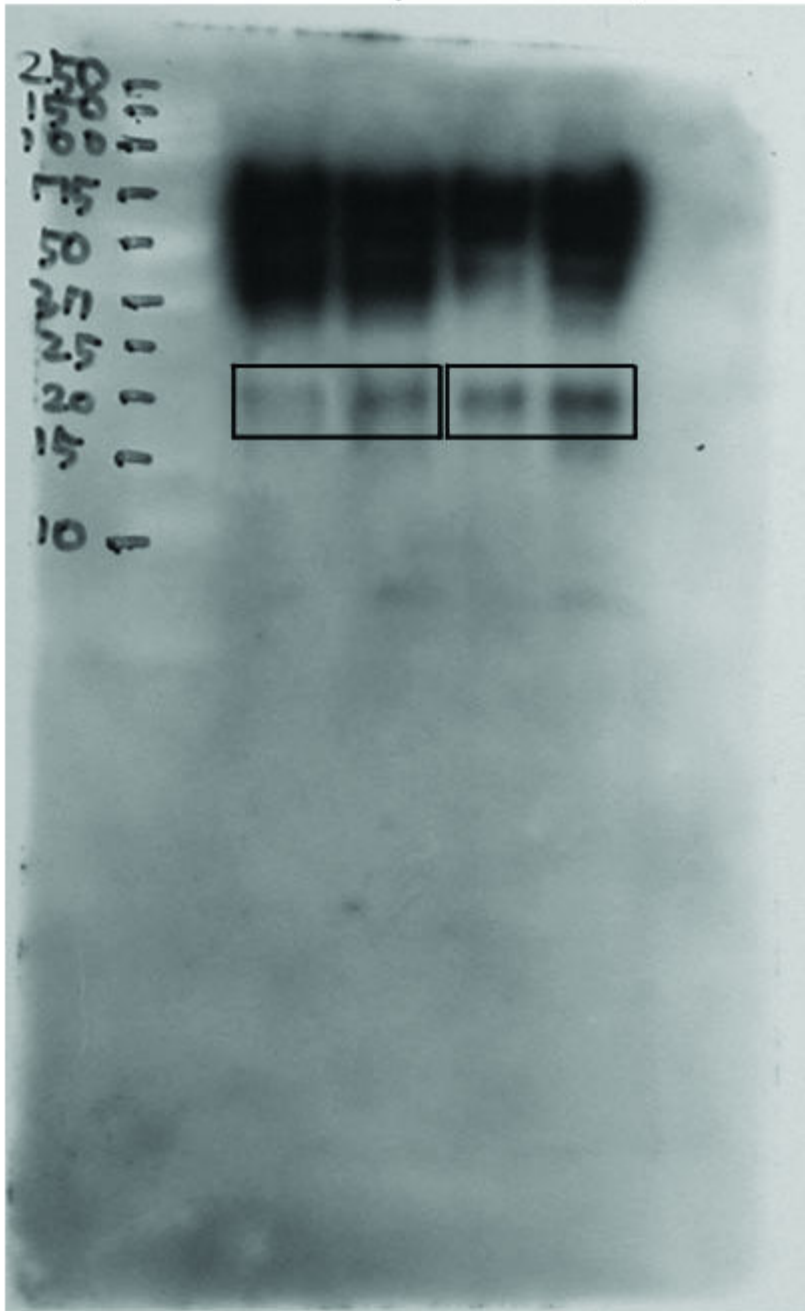


# Supplementary Figure S8.



# Supplementary Figure S9.

siCTL siMap1lc3b  
CTL fA $\beta$  CTL fA $\beta$



siMap1lc3b siCTL  
CTL fA $\beta$  CTL fA $\beta$

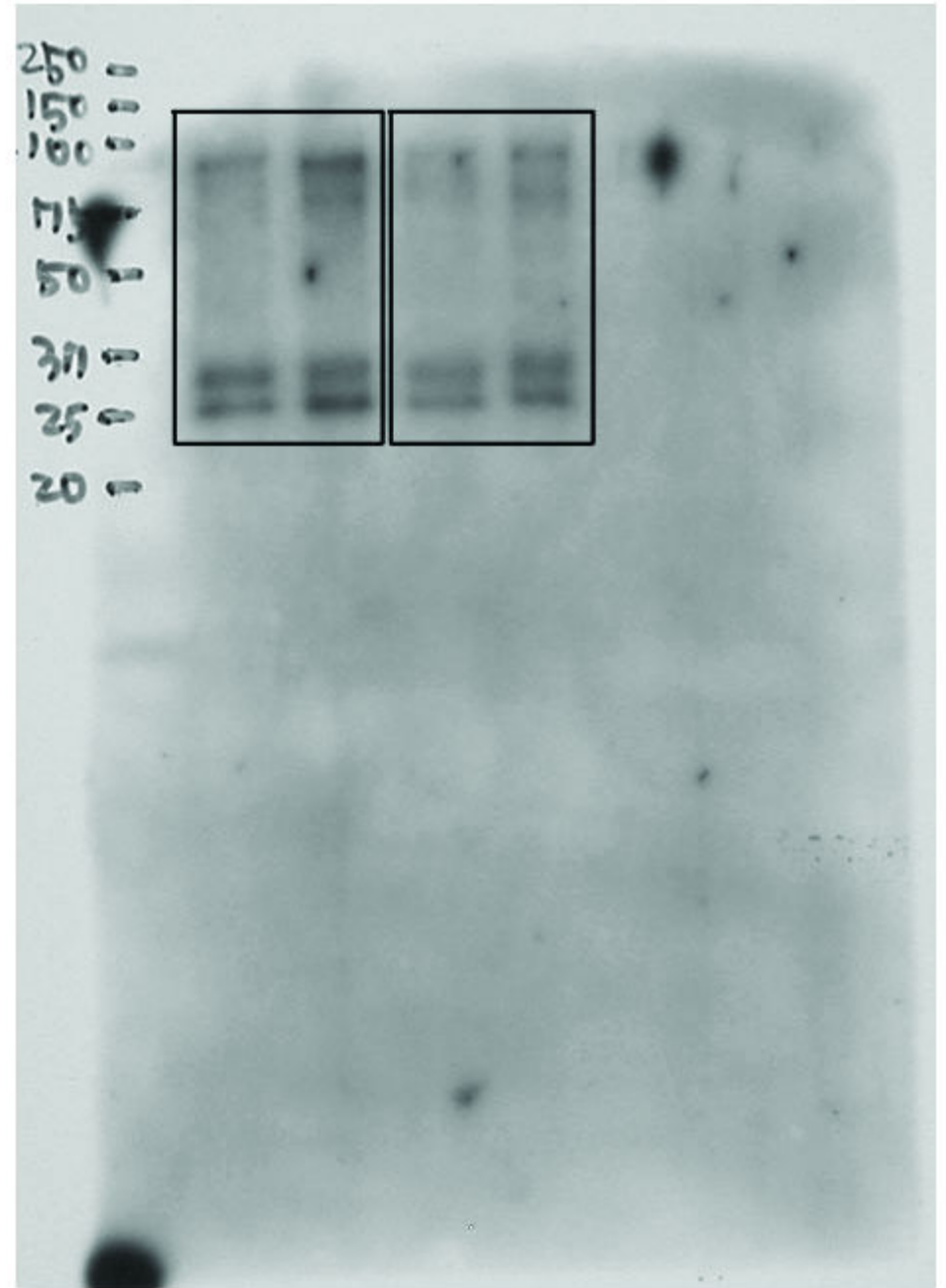


Figure 4 A. CASP1 original blot. Figure 4 A. PYCARD original blot.

## Supplementary Figure Legends

**Figure S1.** Generation of A $\beta$  fibrils *in vitro* and degradation of extracellular A $\beta$  fibrils by microglia. **(A)** Amyloid  $\beta$ -protein<sub>1-42</sub> (A $\beta$ <sub>1-42</sub>) was incubated to a final concentration of 50  $\mu$ M in conditioning medium for 24 h at 37 °C (fA $\beta$  solution). After 24 h, this solution and 50  $\mu$ M monomer A $\beta$  solution (mA $\beta$ ) were diluted to a final concentration of 1  $\mu$ M and added thioflavin S to a final concentration of 20  $\mu$ M. Photographs of thioflavin S-stained solution, showing that the signals were appeared in fA $\beta$  solution, but not in mA $\beta$  solution. Thioflavin S signals are measured in a spectrofluorimeter VICTOR X4. The bar graphs show the fluorescence intensity and the intensity was increased in fA $\beta$  solution than in mA $\beta$  solution. **(B)** After preparation of A $\beta$  fibrils (fA $\beta$ ), western blot was done with a gradient gel of non-reducing condition to see the aggregated patterns of fA $\beta$ . Immunoblot of A $\beta$  with 6E10 antibody shows that smear bands remaining on top of the gel appear in fA $\beta$  lane to reveal A $\beta$  was well fibrillized in the experiments. Monomeric A $\beta$  (mA $\beta$ ) mostly appears lower than 10 kDa. **(C)** Western blot with a gradient gel of non-reducing condition from fA $\beta$ -treated BV2 cell lysates was done with 6E10 antibody to see whether the bands lower than 10 kDa of the main figures reflect the A $\beta$  fibrils well. Immunoblot shows that the higher bands around 250 kDa are well correlated with the lower bands around 10 kDa. **(D)** Photographs of the BV2 microglial cells treated with 1  $\mu$ M of FITC-labeled A $\beta$  fibrils and then stained with cholera toxin B shows that FITC-labeled A $\beta$  was internalized in the cytosols. **(E)** Photographs of the BV2 microglial cell line and primary mouse microglia that were treated with 1  $\mu$ M of FITC-labeled A $\beta$  fibrils for 2 or 24 h, showing that FITC-A $\beta$  fibrils were decreased at 24 hours because they were phagocytosed and degraded by microglia. Phagocytosed FITC-A $\beta$  appears in its punctate form in the cytosol of the microglia. Scale bar, 10  $\mu$ m. **(F)** Western blot

analysis of the lysates and medium of the BV2 and primary microglia treated with A $\beta$  fibrils for the indicated times demonstrates that the intracellular A $\beta$  concentration decreased in a time-dependent manner in the microglia and media. The bar graphs show the densitometric quantification of the immunoblot bands. Each graph shows the band densities of the immunoreactive proteins as a percentage of the density measured at 2 hours (100%). Data are presented as the mean  $\pm$  SEM of 3 independent experiments and were analyzed using the Student t test. \*\* $P < 0.01$ , \*\*\* $P < 0.005$  vs. control.

**Figure S2.** Relationship between the various endosomal-lysosomal compartments with fA $\beta$ . Photographs of the BV2 microglial cells treated with 1  $\mu$ M of FITC-labeled A $\beta$  fibrils and then stained with EEA1 (early endosome antigen 1) for early endosomes, RAB7 for late endosomes and LAMP2 (lysosomal-associated membrane protein 2) for lysosomes show that A $\beta$  is colocalized with each markers in some parts (arrows) and not colocalized in other parts (arrowheads). This may reflect the various stages of A $\beta$  degradation after its phagocytosis.

**Figure S3.** Transfection efficiency of siRNA in BV2 and primary microglia. The transfection efficiency of siRNA in BV2 and primary microglia were examined by FITC-labeled scrambled siRNA. After 24 h of transfection, the efficiency was about 40% in BV2 and about 55% in primary microglia.

**Figure S4.** Unmodified level of A $\beta$ -degrading enzyme. IDE immunoblots of cell lysates that were transfected with the indicated siRNAs. The levels were not changed in siRNA-transfected BV2 and primary microglia. The bar graphs show the densitometric quantification of the immunoblot bands. Each graph shows the band densities of the immunoreactive proteins as a percentage of CTL (100%). Data are presented as the means  $\pm$  SEM of 3

independent experiments and were analyzed using the Student t test. \* $P < 0.05$ , \*\* $P < 0.01$ , \*\*\* $P < 0.005$  vs. control.

**Figure S5.** Increased MAP1LC3B lipidation by AICAR and metformin. BV2 microglial cells were treated with AICAR or metformin and whole cell lysates were collected and then analyzed by immunoblotting with MAP1LC3B. The level of MAP1LC3B is increased in AICAR- or metformin-treated BV2. The bar graphs show the densitometric quantification of the immunoblot bands. Each graph shows the band densities of the immunoreactive proteins as a percentage of CTL (100%). Data are presented as the means  $\pm$  SEM of 3 independent experiments and were analyzed using the Student t test. \* $P < 0.05$ , \*\* $P < 0.01$ , \*\*\* $P < 0.005$  vs. control.

**Figure S6.** Impairment of autophagic flow in microglia after prolonged incubation with A $\beta$ . (A) BV2 microglial cell line and primary mouse microglia cells were transfected with *mCherry-GFP-Map1lc3b* construct and treated with the unlabeled A $\beta$  fibrils (1  $\mu$ M) for 2 h and 24 h. Representative images show that both GFP-MAP1LC3B and mCherry-MAP1LC3B fluorescent dots are increased after addition of A $\beta$  fibrils for 24 h. The bar graphs represent number of mCherry-MAP1LC3B or mCherry-GFP-MAP1LC3B puncta per cell. Scale bar = 10  $\mu$ m. (B) Primary mouse microglia cells were treated with the unlabeled A $\beta$  fibrils (1  $\mu$ M) for 2 h and 24 h and stained with DQ-BSA (red). Representative images show that DQ-BSA positive lysosomal dots are decreased after addition of A $\beta$  fibrils for 24 h. The bar graphs represent quantification of fluorescence of DQ-BSA. Each graph displays the DQ-BSA densities as a percentage of that in control (100%). Scale bar = 10  $\mu$ m. (C) BV2 cells were incubated with L-[ $^{14}$ C]valine for 18 h and subsequently more incubated with fA $\beta$  for

indicated times in HBSS supplemented with 10 mM valine. The medium and cell lysate were collected and its radioactivity was measured by liquid scintillation counting. The bar graphs represent the calculated rate of long-lived protein degradation from the ratio of the radioactivity in medium to the radioactivity in the cell lysate. The rates of long-lived protein degradation were decreased after addition of A $\beta$  fibrils for 9 h and 12 h. \* $P$  < 0.05 vs. control.

**Figure S7.** Aggravation of neuronal damage by impaired microglial autophagy. **(A,B)** Primary mouse microglia were transfected with the indicated siRNAs, preactivated with LPS, and treated with A $\beta$  fibrils (1  $\mu$ M) for 24 h. The conditioned media was transferred to the cortical neurons, and these neurons were subsequently stained with a  $\beta$ 3-tubulin-specific antibody **(A)** or observed with phase-contrast microscopy **(B)**. Representative images show that the neurons were degenerated when the fA $\beta$ -treated microglial medium was transferred to these neurons; this effect was more pronounced following the knockdown of *Map1lc3b*. Scale bar = 20  $\mu$ m. **(C)** No obvious toxicity is seen during 24 h after A $\beta$  fibrils (1  $\mu$ M) is directly added to primary cortical neurons.

**Figure S8.** Increased microglial activation in the cortexes of A $\beta$ -injected *Atg7<sup>fllox/fllox</sup>/Lyz2-Cre* mice. **(A,B)** Cortical sections of the stereotaxically injected *Atg7<sup>fllox/fllox</sup>/Lyz2-Cre* and *Atg7<sup>fllox/fllox</sup>* mice were double-immunostained with AIF-1 (red) and 6E10 (green). Representative images **(B,C)** show that microglia are associated with A $\beta$  in the cortexes of fA $\beta$ -injected *Atg7<sup>fllox/fllox</sup>/Lyz2-Cre* and *Atg7<sup>fllox/fllox</sup>* mice. **(D)** Bar graphs showing the number of A $\beta$ -positive microglia. There is a higher number of microglia, including those containing A $\beta$ , in fA $\beta$ -injected *Atg7<sup>fllox/fllox</sup>/Lyz2-Cre* mice in comparison with fA $\beta$ -injected *Atg7<sup>fllox/fllox</sup>* mice. Data are presented as the means  $\pm$  SEM of 17 samples and were analyzed using the Student *t* test. \*\* $P$  < 0.01, \*\*\* $P$  < 0.005 vs. fA $\beta$ -injected *Atg7<sup>fllox/fllox</sup>* mice.

**Figure S9.** Original blots for cleaved CASP1 and PYCARD in Figure 4A. Immunoblots in Figure 4A were edited for the proper order of samples. Original blots for cleaved CASP1 and PYCARD in Figure 4A are displayed here.